Twinning in 5-fluorosalicylic acid: description of a new polymorph

Martin Lutz,* Jara F. Vliem and Hendrik P. Rodenburg

Crystal and Structural Chemistry, Bijvoet Center for Biomolecular Research, Faculty of Science, Utrecht University, Padualaan 8, 3584 CH Utrecht, The Netherlands. *Correspondence e-mail: m.lutz@uu.nl

The crystal structure of 5-fluorosalicylic acid is known from the literature [Choudhury & Guru Row (2004). *Acta Cryst.* **E60**, o1595–o1597] as crystallizing in the monoclinic crystal system with space-group setting $P2_1/n$ and with one molecule in the asymmetric unit (polymorph I). We describe here a new polymorph which is again monoclinic but with different unit-cell parameters (polymorph II). Polymorph II has two molecules in the asymmetric unit. Its structure was modelled as a twin, with a pseudo-orthorhombic *C*-centred twin cell.

1. Introduction

The current study was undertaken in the context of inter-molecular interactions with fluorine (Dunitz & Taylor, 1997; Chopra & Guru Row, 2011). Surprisingly, we found a new polymorph of 5-fluorosalicylic acid which will be described here.
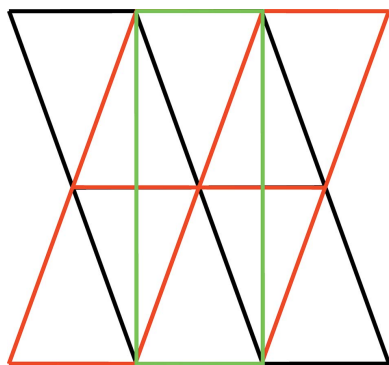
5-Fluorosalicylic acid
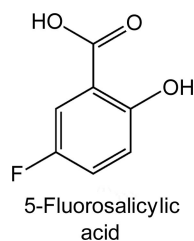
2. Experimental

2.1. Synthesis and crystallization

5-Fluorosalicylic acid was purchased in crystalline form from Sigma–Aldrich and was used directly without recrystallization.

2.2. Refinement

Crystal data, data collection and structure refinement details are summarized in Table 1. All H atoms were located in difference Fourier maps and refined using a riding model, with C—H = 0.95 Å and O—H = 0.84 Å. H-atom displacement parameters were related, with $U_{iso}(H) = 1.2U_{eq}(C)$ for CH or $1.5U_{eq}(O)$ for OH groups. The hydroxy H atoms were allowed to change the torsion angle (instruction AFIX 147 in *SHELXL2017*; Sheldrick, 2015*b*).

Data collection at 110 (2) K consisted of one φ scan with an exposure time of 20 s/image and seven ω scans with an exposure time of 60 s/image. A single orientation matrix was used for the integration of the twinned data with *EVAL15* (Schreurs *et al.*, 2010). A large isotropic mosaicity of 1.7° was used for the prediction of the reflection profiles. In the
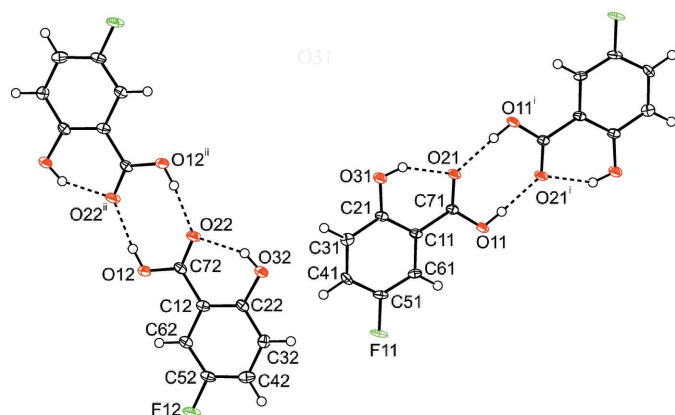
Figure 1
The formation of acid dimers in polymorph II of 5-fluorosalicylic acid, viewed along the b axis. Displacement ellipsoids are drawn at the 50% probability level and H atoms are drawn as small spheres of arbitrary radii. [Symmetry codes: (i) $-x + 1$, $-y + 1$, $-z$; (ii) $-x$, $-y$, $-z$.]

Table 1
Experimental details.

Crystal data	
Chemical formula	$C_7H_5FO_3$
M_r	156.11
Crystal system, space group	Monoclinic, $P2_1/c$
Temperature (K)	110
a, b, c (Å)	23.1729 (14), 3.6802 (3), 15.6312 (8)
β (°)	109.728 (6)
V (Å^3)	1254.79 (15)
Z	8
Radiation type	Mo $K\alpha$
μ (mm^{-1})	0.15
Crystal size (mm)	$0.27 \times 0.21 \times 0.04$
Data collection	
Diffractometer	Bruker Kappa APEXII
Absorption correction	Numerical (*SADABS*; Krause *et al.*, 2015)
T_{min}, T_{max}	0.694, 1.000
No. of measured, independent and observed [$I > 2\sigma(I)$] reflections	30602, 2884, 2386
R_{int}	0.064
$(\sin \theta/\lambda)_{max}$ (Å^{-1})	0.649
Refinement	
$R[F^2 > 2\sigma(F^2)]$, $wR(F^2)$, S	0.047, 0.123, 1.05
No. of reflections	2884
No. of parameters	204
H-atom treatment	H-atom parameters constrained
$\Delta\rho_{max}, \Delta\rho_{min}$ (e Å^{-3})	0.57, -0.27

Computer programs: *APEX3* (Bruker, 2016), *PEAKREF* (Schreurs, 2016), *EVAL15* (Schreurs *et al.*, 2010), *SADABS* (Krause *et al.*, 2015), *SHELXT* (Sheldrick, 2015a), *SHELXL2017* (Sheldrick, 2015b), *PLATON* (Spek, 2009) and *publCIF* (Westrip, 2010).

structure refinement with *SHELXL2017*, a TWIN instruction with the matrix ($101/0\bar{1}0/00\bar{1}$) was included. (The matrix gives the transformation of real axes and reciprocal indices of the first component to those of the second.) The resulting twin fraction was BASF = 0.495 (2), the fraction corresponding to the second component. While the agreement factors of the least-squares refinement are acceptable, a **TLS** analysis with the *THMA11* software (Schomaker & Trueblood, 1998) indicates some nonrigid behaviour of the two independent molecules. This can be interpreted as slight shortcomings of the data quality. Still, restraining the atomic displacement parameters was not considered necessary.

The temperature-dependent measurements were performed on 360° φ scans with a fixed detector distance on the same crystal as was used in the full structure analysis.

3. Results and discussion

3.1. Similarities in the two polymorphs

The literature structure of 5-fluorosalicylic acid (polymorph I) was reported in the space-group setting $P2_1/n$ and is characterized by the formation of a typical centrosymmetric $R_2^2(8)$ acid dimer (Choudhury & Guru Row, 2004). The same dimer formation is found in the current study of polymorph II

(Fig. 1). The strength of the hydrogen bonds in the acid dimers is comparable in both polymorphs. An essential planarity of the molecules is also common to both polymorphs, which are stabilized by an intramolecular hydrogen bond from the hydroxy group to the carboxylic acid group. The molecular symmetry is then approximately C_s. In polymorph I, a dihedral angle of 4.0 (1)° was found between the planes of the carboxylic acid group and the phenyl ring (Choudhury & Guru Row, 2004). In polymorph II, there are two independent molecules and the corresponding dihedral angles are 1.4 (3) and 4.7 (3)° (for torsion angles, see Table 2). The difference between the two polymorphs is thus not in the molecular conformation but in the packing of the acid dimers.
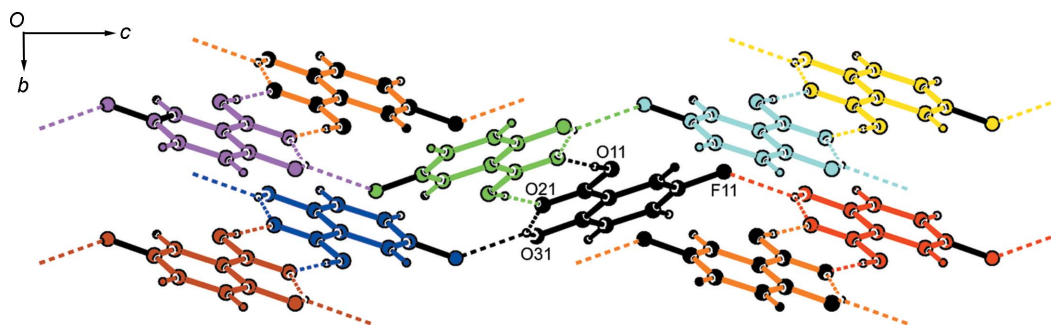

Figure 2
The two-dimensional hydrogen-bonded layer of one independent molecule of polymorph II, viewed along the a axis. The second independent molecule has the same hydrogen-bonding topology, but with a longer O—H···F distance.

Table 2
Selected geometric parameters (Å, °).

F11—C51	1.369 (3)	F12—C52	1.367 (3)
O11—C71	1.314 (3)	O12—C72	1.316 (3)
O21—C71	1.240 (3)	O22—C72	1.236 (3)
O31—C21	1.353 (3)	O32—C22	1.356 (3)
C61—C11—C71—O21	−179.1 (3)	C22—C12—C72—O22	−4.6 (4)
C21—C11—C71—O21	2.1 (4)	C62—C12—C72—O22	175.3 (2)
C61—C11—C71—O11	0.6 (4)	C22—C12—C72—O12	175.4 (2)
C21—C11—C71—O11	−178.3 (2)	C62—C12—C72—O12	−4.7 (4)

Table 3
Hydrogen-bond geometry (Å, °).

Reflection data from one φ and seven ω scans.

$D-H\cdots A$	$D-H$	$H\cdots A$	$D\cdots A$	$D-H\cdots A$
O11—H11O$\cdots$O21[i]	0.84	1.81	2.643 (3)	176
O31—H31O$\cdots$O21	0.84	1.90	2.620 (3)	144
O31—H31O$\cdots$F11[ii]	0.84	2.38	3.028 (3)	134
O12—H12O$\cdots$O22[iii]	0.84	1.83	2.659 (3)	168
O32—H32O$\cdots$O22	0.84	1.88	2.597 (3)	143
O32—H32O$\cdots$F12[iv]	0.84	2.64	3.287 (3)	135

Symmetry codes: (i) $-x+1, -y+1, -z$; (ii) $x, -y+\frac{3}{2}, z-\frac{1}{2}$; (iii) $-x, -y, -z$; (iv) $x, -y+\frac{1}{2}, z-\frac{1}{2}$.

3.2. Hydrogen bonding

Polymorph I (Choudhury & Guru Row, 2004) and polymorph II (current study) are both characterized by centrosymmetric $R_2^2(8)$ acid dimers. Polymorph I has one molecule in the asymmetric unit and polymorph II has two. In polymorph I, the centre of the acid dimer is on $(\frac{1}{2}, 1, 1)$ (Wyckoff position d). In polymorph II, the centres of the two independent molecules are on $(\frac{1}{2}, \frac{1}{2}, 0)$ and $(0, 0, 0)$ (Wyckoff positions d and a, respectively).

In addition to the intramolecular hydrogen bond to the carboxylic acid group, the hydroxy group is involved in an intermolecular hydrogen bond to the organic fluorine of a neighbouring molecule. Overall, this can be described as a bifurcated situation (Jeffrey, 1997). In polymorph I, the acceptor molecule is related by a simple translation. The O—H$\cdots$F interactions consequently lead to a one-dimensional hydrogen-bonded chain in the c direction. In polymorph II, the acceptor molecules are related by glide planes and the O—H$\cdots$F interactions lead to two-dimensional hydrogen-bonded layers parallel to the bc plane (Fig. 2 and Table 3). This two-dimensional arrangement can also be seen in the external shape of the crystals, which are thin plates with hkl = (100) as the predominant face. The O31—H31O$\cdots$F11[ii] hydrogen bond in polymorph II is slightly shorter [O$\cdots$F = 3.028 (3) Å] and the O32—H32O$\cdots$F12[iv] hydrogen bond significantly longer [O$\cdots$F = 3.287 (3) Å] than O3—H3O$\cdots$F1 in polymorph I [O$\cdots$F = 3.107 (2) Å]. The O$\cdots$F distance of 3.287 (3) Å in polymorph II is longer than the sum of the van der Waals radii (2.99 Å), but because the packing topology is similar to that of the other independent molecule, we still consider this an important interaction.

Polymorph II at 110 (2) K has a calculated density of 1.653 Mg m^{-3} and a packing index of 74.9% (Kitajgorodskij, 1973), while polymorph I at 293 K has a density of 1.589 Mg m^{-3} and a packing index of 71.6%. At room temperature, polymorph II will still have a higher density and higher packing index than polymorph I if the temperature-dependent unit-cell parameters (Table 4) are used for an extrapolation. According to the density rule (Kitaigorodskii, 1961), this could indicate a higher stability of polymorph II, but we have to keep in mind the warning of Bernstein (2002) about the missing accuracy of unit-cell determinations. In the present case, the inaccuracy might even be higher because of pseudomerohedral twinning and the consequently smeared-out reflection profiles.
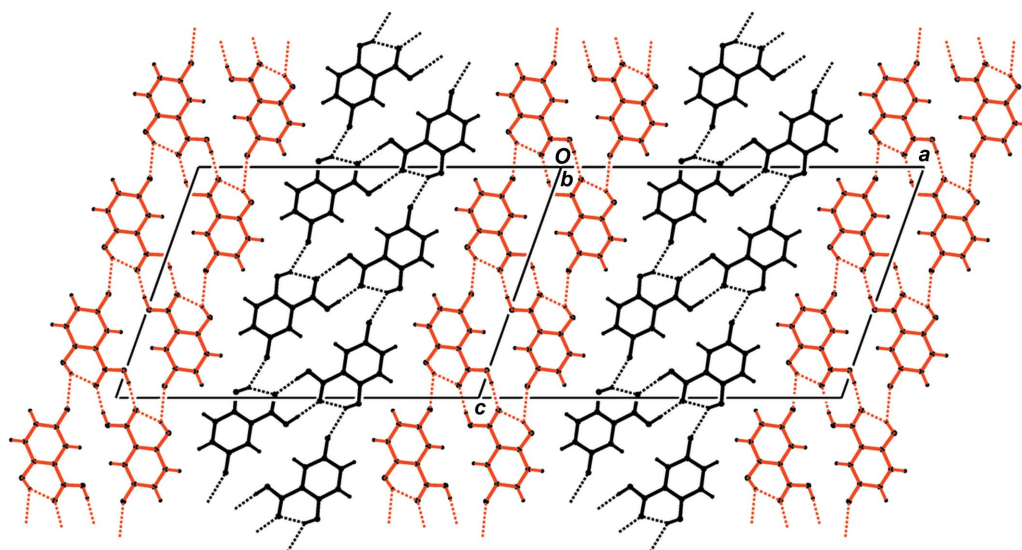
Figure 3
The two-dimensional hydrogen-bonded layers in the bc plane, viewed along the b axis. The layers are stacked in the a direction. The two independent molecules are drawn in black and red.
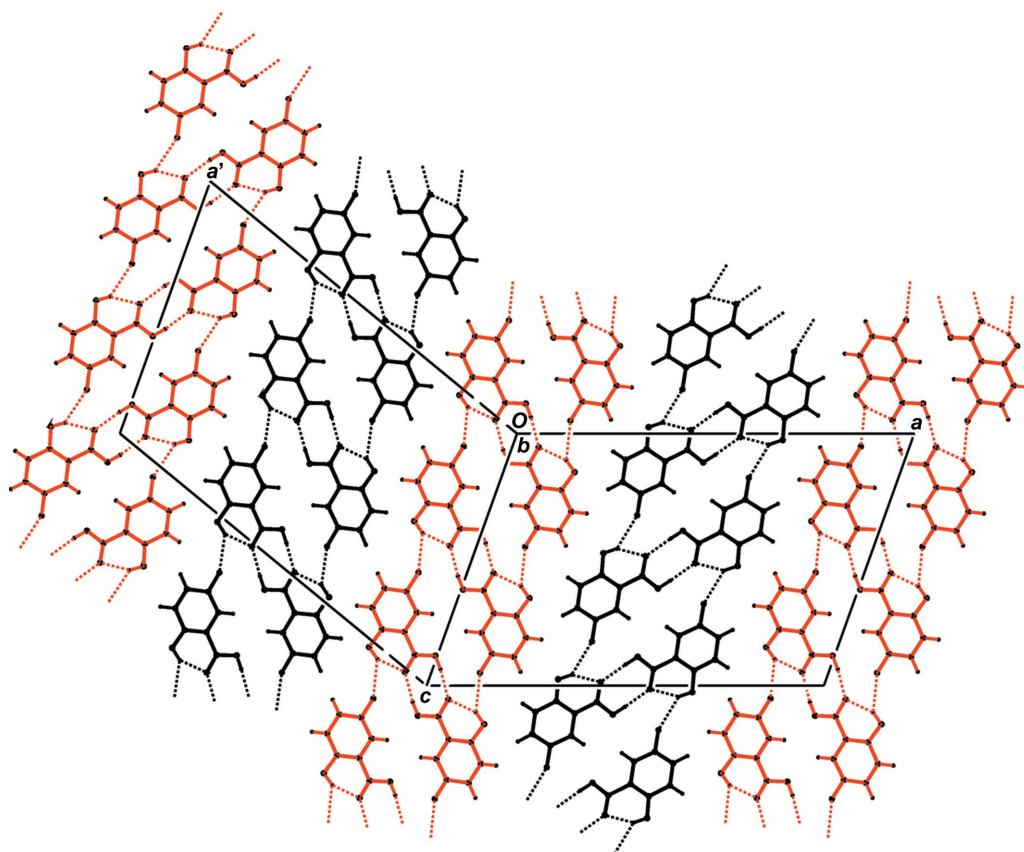
Figure 4
Artistic impression of the twinned crystal structure. The two independent molecules are drawn in black and red, respectively. Stacking faults are proposed as the underlying cause of the twinning. A twofold rotation about the *c* axis is assumed as the twin operation.

3.3. Pseudo-orthorhombic twinning

The structure of polymorph II is based on two-dimensional hydrogen-bonded layers (§3.2, *Hydrogen bonding*). These layers are stacked on top of each other in the *a* direction (Fig. 3). Stacking faults in this direction may occur easily, thereby interrupting the three-dimensional translation symmetry of the lattice. The consequence is a twinned crystal structure with a twofold rotation about the *c* axis as a twin operation (Fig. 4). For the X-ray intensities in the monoclinic crystal system, this is equivalent to a twofold rotation about hkl = (100) in reciprocal space. In the current centrosymmetric space group, the mirror operations perpendicular to the direct *c* axis and to the reciprocal *a** axis are equivalent twin operations as well. Of these four possibilities, we arbitrarily

chose the matrix $(101/0\bar{1}0/00\bar{1})$ for the least-squares refinement. This twin matrix corresponds to a twofold rotation about hkl = (100) or uvw = [201]. Twin refinement ended in a twin fraction of 0.495 (2) for the second component.

The application of the described twin law results in a pseudo-orthorhombic *C*-centred twin lattice (Fig. 5). The transformation matrix between the monoclinic *P*-cell and the orthorhombic *C*-cell is $(00\bar{1}/201/0\bar{1}0)$, resulting in an angle γ = 89.983°, based on 15239 reflections from eight scans. The twin obliquity (Le Page, 2002) is consequently 0.017°. All reflections are overlapping and the data can be integrated with a single orientation matrix. The twin matrix can be introduced later in the structure refinement.

Because of the approximately 50% twin fraction, the averaging *R* value for the orthorhombic symmetry (R_{int} = 0.047) is

Table 4
Temperature-dependent unit-cell parameters of polymorph II.

The crystal was cooled from 210 (2) to 110 (2) K in steps of 20 K. Unit-cell parameters were obtained from 360° φ scans by post-refinement of integrated data with *EVAL15* (4148–5093 reflections for unit-cell determination; Schreurs *et al.*, 2010). The detector position was kept fixed during the measurement.

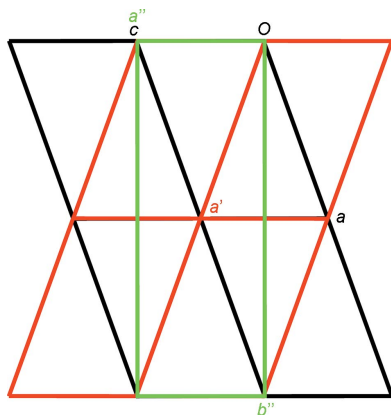| T (K)	a (Å)	b (Å)	c (Å)	β (°)	V (Å^3)	Twin obliquity (°)
210 (2)	23.241 (4)	3.7219 (10)	15.684 (2)	109.742 (9)	1276.9 (5)	0.022
190 (2)	23.229 (5)	3.7120 (9)	15.6765 (18)	109.750 (10)	1272.2 (4)	0.029
170 (2)	23.215 (4)	3.7031 (6)	15.6654 (15)	109.765 (8)	1267.4 (3)	0.047
150 (2)	23.201 (3)	3.6943 (5)	15.6528 (11)	109.759 (7)	1262.6 (2)	0.045
130 (2)	23.189 (3)	3.6864 (5)	15.6401 (13)	109.746 (8)	1258.3 (2)	0.038
110 (2)	23.180 (3)	3.6795 (4)	15.6317 (17)	109.735 (8)	1254.9 (3)	0.030

Figure 5
The twin relationship between the monoclinic lattices drawn in black and red. The pseudo-orthorhombic C-centred twin cell is drawn in green.

Table 5
Reflection conditions in the twinned data set.

Reflection indices are based on the orthorhombic unit-cell setting, with $a = 15.63$, $b = 43.63$ and $c = 3.68$ Å. Reflection intensities were derived from the calculated structure factors with the twin law applied and a perfect twin fraction of 50%.

hkl	$h + k = 2n$	$hk0$	$h + k = 2n$
$0kl$	$k = 2n$	$h00$	$h = 2n$
$h0l$	$h = 2n$	$0k0$	$k = 2n$
$hk0$	$h = 2n$	$00l$	$l = 2n$
$hk0$	$k = 2n$		

similar to the low value for the monoclinic symmetry ($R_{int} = 0.044$). A distinction between the two symmetries cannot be made on this basis. A strong indication that the symmetry is not orthorhombic is the systematic absences of the twinned reflection data which are incompatible with any orthorhombic space group (Table 5). Additionally, all attempts failed to solve the structure in C-centred orthorhombic cells.

Space-group incompatible absences are not only an indication for a lowering of the symmetry but also of the presence of twinning (Herbst-Irmer & Sheldrick, 1998). Twinning in reflection data can often also be detected by an analysis of the $|E^2 - 1|$ value. In the present case, this value is 0.78, which is not a very strong indication of twinning.
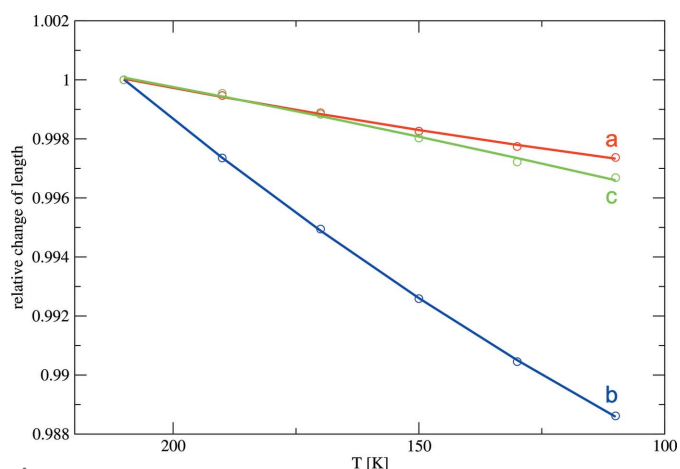

Figure 6
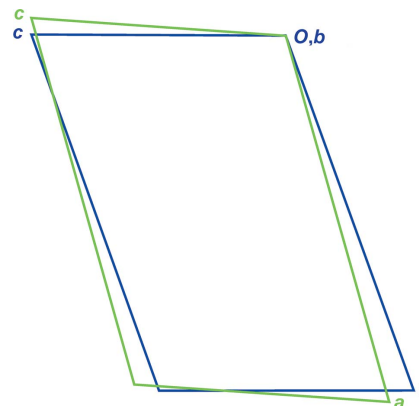Change of axis lengths during cooling in polymorph II.

Figure 7
Orientation of the crystal axes on the X-ray diffractometer (laboratory coordinate system). The blue unit cell is at a temperature of 110 (2) K and the green unit cell at 210 (2) K. Both unit-cell drawings are derived from the corresponding orientation matrices (given in the CIF files in the supporting information).

3.4. Thermal expansion

Polymorph II was subjected to a temperature-dependent unit-cell determination by cooling from 210 to 110 K in steps of 20 K. The results are shown in Table 4 and Fig. 6. The twin obliquity is very low on the whole temperature range and the twinning does not lead to a splitting of the reflections. Single-crystal-type unit-cell determinations are therefore possible. Due to the layered packing and the plate shape of the crystal, a rather large mosaicity had to be used to predict the reflection profiles. Analysis of the temperature dependence shows that the largest relative change is in the direction of the monoclinic b axis.

The temperature-dependent unit-cell data can be used to calculate the thermal expansion tensor. This is a symmetrical second-rank tensor that is expressed in a Cartesian system (Lovett, 1999). With monoclinic symmetry, only four of its components are independent. Using the algorithm of Ohashi (1982), as implemented in the $PLATON$ software (Spek, 2009), the following unit strain tensor was calculated between the temperatures of 110 and 210 K: $(26.4, 0, -1.8/0, 115.2, 0/-1.8, 0, 32.8)$ [$\times 10^{-6}$].

An eigenvector/eigenvalue analysis shows that one eigenvector is perfectly aligned with the monoclinic b axis, as

Table 6
Temperature-dependent intermolecular hydrogen-bond distances.

Reflection data were obtained from 360° φ scans with a fixed detector distance (see Table 4). Refinement results are given in the CIF files in the supporting information.

T (K)	$O11 \cdots O21^i$	$O12 \cdots O22^{iii}$	$O31 \cdots F11^{ii}$	$O32 \cdots F12^{iv}$
210 (2)	2.645 (5)	2.661 (5)	3.054 (5)	3.322 (6)
190 (2)	2.648 (5)	2.660 (5)	3.050 (5)	3.315 (5)
170 (2)	2.652 (4)	2.657 (5)	3.047 (4)	3.307 (5)
150 (2)	2.643 (4)	2.659 (4)	3.044 (4)	3.297 (4)
130 (2)	2.645 (4)	2.658 (4)	3.037 (4)	3.294 (4)
110 (2)	2.647 (4)	2.659 (4)	3.030 (3)	3.287 (4)

Symmetry codes: (i) $-x + 1, -y + 1, -z$; (ii) $x, -y + \frac{3}{2}, z - \frac{1}{2}$; (iii) $-x, -y, -z$; (iv) $x, -y + \frac{1}{2}, z - \frac{1}{2}$.
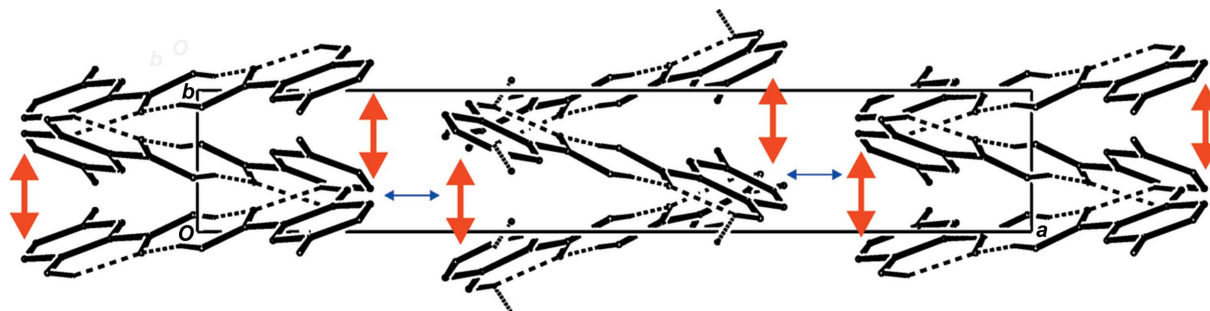
Figure 8
Thermal expansion affects the hydrogen-bonded zigzag layers in the *bc* plane more (red arrows) than in the perpendicular direction (blue arrows). Thermal expansion is similar along the *c* and *a* axes. C—H hydrogens have been omitted for clarity.

required by symmetry. This vector corresponds to the largest strain [115 (3) $\times$ 10^{-6} K^{-1}]. The two perpendicular eigenvectors form angles of 5 and 15° with the crystallographic *a* and *c* axes, respectively. Their eigenvalues in the *ac* plane are approximately the same, with values of 33.3 (17) and 26 (2) $\times$ 10^{-6} K^{-1}.

A consequence of the eigenvector directions is a pseudo-rotation of the crystal on the X-ray diffractometer during the temperature change. This is shown in Fig. 7 and is quite significant. The pseudo-rotation angle between 110 (2) and 210 (2) K is approximately 4.3° and roughly about the *b* axis.

Polymorph II forms hydrogen-bonded layers in the *bc* plane (§3.2, *Hydrogen bonding*). Intuitively, one would thus expect the largest thermal expansion in the direction of the *a* axis. A closer look at the packing shows that the hydrogen-bonded planes are in a zigzag arrangement (Fig. 8). By increasing the temperature, the joints of this 'accordion'-type layout are expanded, while the perpendicular stacking direction is only very slightly temperature sensitive. It is known from the literature that layered structures can even have a uni-axial negative thermal expansion (Bhattacharya & Saha, 2012). In the present case, we still observe a very small positive expansion. Recent research has demonstrated the importance of dispersive interactions to fully explain phenomena of thermal expansion (Dove & Fang, 2016). With the absence of strong intermolecular bonds in the *a* direction, one could speculate about an influence of dispersive forces here too.

Thermal expansion analysis can provide insight into the strengths of intermolecular interactions (Salud *et al.*, 1998). An analysis of the intermolecular hydrogen-bond distances in the present case (Table 6) shows that the O—H$\cdots$O interactions are insensitive to the temperature change between 210 and 110 K. This is consistent with strong hydrogen bonding, and the acid dimers can indeed be considered the building units of both polymorphs. The temperature dependence differs between the two symmetry-independent O—H$\cdots$F hydrogen bonds. The O32$\cdots$F12[iv] distance is not only longer than O31$\cdots$F11[ii], it is also more sensitive to the temperature change. By linear regression, a slope of 3.5 $\times$ 10^{-4} K^{-1} for O32$\cdots$F12[iv] is obtained *versus* 2.3 $\times$ 10^{-4} K^{-1} for O31$\cdots$F11[ii]. The different strengths of the two O—H$\cdots$F hydrogen bonds is thus consistently proven.

References

Bernstein, J. (2002). *Polymorphism in Molecular Crystals*, pp. 40–41. Oxford: Clarendon Press.
Bhattacharya, S. & Saha, B. K. (2012). *Cryst. Growth Des.* **12**, 4716–4719.
Bruker (2016). *APEX3*. Bruker AXS Inc., Madison, Wisconsin, USA.
Chopra, D. & Guru Row, T. N. (2011). *CrystEngComm*, **13**, 2175–2186.
Choudhury, A. R. & Guru Row, T. N. (2004). *Acta Cryst.* E**60**, o1595–o1597.
Dove, M. T. & Fang, H. (2016). *Rep. Prog. Phys.* **79**, 066503.
Dunitz, J. D. & Taylor, R. (1997). *Chem. Eur. J.* **3**, 89–98.
Herbst-Irmer, R. & Sheldrick, G. M. (1998). *Acta Cryst.* B**54**, 443–449.
Jeffrey, G. A. (1997). *An Introduction to Hydrogen Bonding*, pp. 21–26. Oxford University Press.
Kitaigorodskii, A. I. (1961). In *Organic Chemical Crystallography*. New York: Consultants Bureau.
Kitajgorodskij, A. I. (1973). In *Molecular Crystals and Molecules*. New York: Academic Press.
Krause, L., Herbst-Irmer, R., Sheldrick, G. M. & Stalke, D. (2015). *J. Appl. Cryst.* **48**, 3–10.
Le Page, Y. (2002). *J. Appl. Cryst.* **35**, 175–181.
Lovett, D. R. (1999). In *Tensor Properties of Crystals*, 2nd ed. Bristol and Philadelphi: Institute of Physics Publishing.
Ohashi, Y. (1982). *Comparative Crystal Chemistry*, edited by R. M. Hazen & L. W. Finger, pp. 92–102. Chichester: Wiley-Interscience.
Salud, J., Barrio, M., López, D. O., Tamarit, J. L. & Alcobé, X. (1998). *J. Appl. Cryst.* **31**, 748–757.
Schomaker, V. & Trueblood, K. N. (1998). *Acta Cryst.* B**54**, 507–514.
Schreurs, A. M. M. (2016). *PEAKREF*. University of Utrecht, The Netherlands.
Schreurs, A. M. M., Xian, X. & Kroon-Batenburg, L. M. J. (2010). *J. Appl. Cryst.* **43**, 70–82.
Sheldrick, G. M. (2015a). *Acta Cryst.* A**71**, 3–8.
Sheldrick, G. M. (2015b). *Acta Cryst.* C**71**, 3–8.
Spek, A. L. (2009). *Acta Cryst.* D**65**, 148–155.
Westrip, S. P. (2010). *J. Appl. Cryst.* **43**, 920–925.

Twinning in 5-fluorosalicylic acid: description of a new polymorph

Martin Lutz, Jara F. Vliem and Hendrik P. Rodenburg

Computing details

Data collection: *APEX3* (Bruker, 2016); cell refinement: *PEAKREF* (Schreurs, 2016); data reduction: *EVAL15* (Schreurs *et al.*, 2010) and *SADABS* (Krause *et al.*, 2015); program(s) used to solve structure: SHELXT (Sheldrick, 2015a); program(s) used to refine structure: *SHELXL2017* (Sheldrick, 2015b); molecular graphics: *PLATON* (Spek, 2009); software used to prepare material for publication: *publCIF* (Westrip, 2010).

5-Fluorosalicylic acid

Crystal data

$C_7H_5FO_3$	$F(000) = 640$
$M_r = 156.11$	$D_x = 1.653$ Mg m^{-3}
Monoclinic, $P2_1/c$	Mo $K\alpha$ radiation, $\lambda = 0.71073$ Å
$a = 23.1729$ (14) Å	Cell parameters from 15239 reflections
$b = 3.6802$ (3) Å	$\theta = 1.8$–27.5°
$c = 15.6312$ (8) Å	$\mu = 0.15$ mm^{-1}
$\beta = 109.728$ (6)°	$T = 110$ K
$V = 1254.79$ (15) Å^3	Plate, colourless
$Z = 8$	$0.27 \times 0.21 \times 0.04$ mm

Data collection

Bruker Kappa APEXII diffractometer	2884 independent reflections
Radiation source: sealed tube	2386 reflections with $I > 2\sigma(I)$
φ and ω scans	$R_{int} = 0.064$
Absorption correction: numerical (*SADABS*; Krause *et al.*, 2015)	$\theta_{max} = 27.5°$, $\theta_{min} = 1.9°$
	$h = -30 \rightarrow 30$
	$k = -4 \rightarrow 4$
$T_{min} = 0.694$, $T_{max} = 1.000$	$l = -20 \rightarrow 19$
30602 measured reflections	

Refinement

Refinement on F^2	Secondary atom site location: difference Fourier map
Least-squares matrix: full	
$R[F^2 > 2\sigma(F^2)] = 0.047$	Hydrogen site location: difference Fourier map
$wR(F^2) = 0.123$	H-atom parameters constrained
$S = 1.05$	$w = 1/[\sigma^2(F_o^2) + (0.0731P)^2 + 0.4868P]$
2884 reflections	where $P = (F_o^2 + 2F_c^2)/3$
204 parameters	$(\Delta/\sigma)_{max} < 0.001$
0 restraints	$\Delta\rho_{max} = 0.57$ e Å^{-3}
Primary atom site location: dual	$\Delta\rho_{min} = -0.27$ e Å^{-3}

Special details

Geometry. All esds (except the esd in the dihedral angle between two l.s. planes) are estimated using the full covariance matrix. The cell esds are taken into account individually in the estimation of esds in distances, angles and torsion angles; correlations between esds in cell parameters are only used when they are defined by crystal symmetry. An approximate (isotropic) treatment of cell esds is used for estimating esds involving l.s. planes.

Refinement. efined as a 2-component twin

Fractional atomic coordinates and isotropic or equivalent isotropic displacement parameters (Å²)

	x	*y*	*z*	U_{iso}*/U_{eq}
F11	0.37637 (8)	0.4284 (5)	0.32426 (10)	0.0235 (4)
O11	0.49467 (9)	0.4087 (5)	0.11432 (12)	0.0198 (5)
H11O	0.518303	0.390822	0.083928	0.030*
O21	0.43470 (9)	0.6756 (6)	−0.01370 (14)	0.0189 (5)
O31	0.32536 (9)	0.9067 (6)	−0.02534 (13)	0.0189 (4)
H31O	0.355419	0.882858	−0.043422	0.028*
C11	0.39756 (12)	0.6221 (7)	0.10943 (18)	0.0137 (5)
C21	0.34068 (12)	0.7843 (7)	0.06108 (19)	0.0139 (6)
C31	0.29715 (12)	0.8263 (7)	0.1037 (2)	0.0170 (6)
H31	0.258631	0.933751	0.071594	0.020*
C41	0.30959 (12)	0.7131 (8)	0.19201 (19)	0.0160 (6)
H41	0.280138	0.745701	0.221390	0.019*
C51	0.36549 (12)	0.5513 (7)	0.23758 (18)	0.0166 (6)
C61	0.40960 (12)	0.5044 (7)	0.19938 (17)	0.0145 (5)
H61	0.447691	0.394723	0.232620	0.017*
C71	0.44369 (12)	0.5704 (7)	0.06512 (18)	0.0138 (5)
F12	0.12270 (8)	−0.1498 (5)	0.44878 (11)	0.0271 (5)
O12	0.00509 (9)	−0.1177 (6)	0.11867 (12)	0.0210 (5)
H12O	−0.020011	−0.100787	0.065548	0.032*
O22	0.06700 (9)	0.1506 (6)	0.05439 (14)	0.0202 (5)
O32	0.17965 (9)	0.2931 (6)	0.15292 (14)	0.0213 (5)
H32O	0.148360	0.312280	0.106257	0.032*
C12	0.10439 (12)	0.0503 (7)	0.21348 (18)	0.0149 (5)
C22	0.16289 (13)	0.1804 (7)	0.2237 (2)	0.0157 (6)
C32	0.20716 (12)	0.1943 (8)	0.3101 (2)	0.0173 (6)
H32	0.247111	0.281184	0.317137	0.021*
C42	0.19354 (14)	0.0831 (8)	0.3856 (2)	0.0207 (6)
H42	0.223687	0.092787	0.444439	0.025*
C52	0.13573 (13)	−0.0412 (7)	0.37363 (18)	0.0172 (6)
C62	0.09072 (12)	−0.0621 (7)	0.29029 (19)	0.0159 (5)
H62	0.051093	−0.150876	0.284567	0.019*
C72	0.05744 (12)	0.0321 (7)	0.12241 (18)	0.0150 (6)

Atomic displacement parameters (Å²)

	U^{11}	U^{22}	U^{33}	U^{12}	U^{13}	U^{23}
F11	0.0365 (10)	0.0293 (9)	0.0086 (9)	−0.0006 (7)	0.0126 (7)	0.0004 (7)
O11	0.0203 (10)	0.0295 (11)	0.0129 (11)	0.0071 (8)	0.0100 (8)	0.0054 (8)

O21	0.0215 (11)	0.0258 (11)	0.0119 (11)	0.0058 (8)	0.0089 (8)	0.0068 (8)
O31	0.0213 (10)	0.0236 (10)	0.0141 (10)	0.0051 (8)	0.0088 (8)	0.0052 (8)
C11	0.0193 (13)	0.0119 (12)	0.0104 (13)	−0.0026 (10)	0.0059 (10)	−0.0022 (9)
C21	0.0204 (13)	0.0105 (12)	0.0117 (14)	−0.0009 (10)	0.0068 (11)	−0.0034 (10)
C31	0.0208 (14)	0.0125 (13)	0.0170 (15)	0.0023 (10)	0.0055 (12)	−0.0004 (10)
C41	0.0185 (12)	0.0168 (13)	0.0175 (14)	−0.0044 (10)	0.0124 (11)	−0.0049 (10)
C51	0.0264 (14)	0.0158 (12)	0.0084 (12)	−0.0058 (11)	0.0068 (11)	−0.0006 (10)
C61	0.0200 (13)	0.0131 (12)	0.0090 (12)	0.0000 (10)	0.0030 (10)	−0.0022 (10)
C71	0.0177 (13)	0.0126 (12)	0.0116 (13)	−0.0008 (10)	0.0058 (10)	−0.0031 (10)
F12	0.0381 (11)	0.0341 (11)	0.0119 (9)	−0.0026 (8)	0.0122 (8)	0.0025 (7)
O12	0.0216 (11)	0.0300 (12)	0.0122 (11)	−0.0046 (8)	0.0066 (8)	0.0000 (8)
O22	0.0263 (11)	0.0238 (11)	0.0129 (11)	−0.0046 (8)	0.0098 (9)	0.0011 (8)
O32	0.0216 (10)	0.0299 (12)	0.0149 (11)	−0.0050 (9)	0.0095 (9)	0.0011 (8)
C12	0.0227 (14)	0.0096 (12)	0.0138 (13)	0.0017 (10)	0.0080 (11)	−0.0012 (9)
C22	0.0202 (14)	0.0125 (13)	0.0175 (15)	−0.0002 (10)	0.0103 (12)	−0.0015 (10)
C32	0.0179 (14)	0.0142 (14)	0.0194 (16)	−0.0029 (10)	0.0056 (12)	−0.0020 (10)
C42	0.0308 (16)	0.0146 (14)	0.0155 (15)	0.0017 (11)	0.0061 (12)	−0.0012 (10)
C52	0.0290 (14)	0.0116 (13)	0.0140 (13)	0.0026 (11)	0.0112 (12)	0.0014 (10)
C62	0.0218 (14)	0.0114 (12)	0.0167 (13)	−0.0003 (10)	0.0095 (12)	−0.0016 (10)
C72	0.0200 (13)	0.0122 (13)	0.0159 (14)	−0.0006 (10)	0.0100 (11)	−0.0011 (10)

Geometric parameters (Å, º)

F11—C51	1.369 (3)	F12—C52	1.367 (3)
O11—C71	1.314 (3)	O12—C72	1.316 (3)
O11—H11O	0.8400	O12—H12O	0.8400
O21—C71	1.240 (3)	O22—C72	1.236 (3)
O31—C21	1.353 (3)	O32—C22	1.356 (3)
O31—H31O	0.8400	O32—H32O	0.8400
C11—C61	1.406 (4)	C12—C22	1.395 (4)
C11—C21	1.411 (4)	C12—C62	1.404 (4)
C11—C71	1.469 (4)	C12—C72	1.473 (4)
C21—C31	1.392 (4)	C22—C32	1.394 (4)
C31—C41	1.376 (4)	C32—C42	1.382 (4)
C31—H31	0.9500	C32—H32	0.9500
C41—C51	1.385 (4)	C42—C52	1.368 (4)
C41—H41	0.9500	C42—H42	0.9500
C51—C61	1.358 (4)	C52—C62	1.369 (4)
C61—H61	0.9500	C62—H62	0.9500
C71—O11—H11O	109.5	C72—O12—H12O	109.5
C21—O31—H31O	109.5	C22—O32—H32O	109.5
C61—C11—C21	120.0 (2)	C22—C12—C62	119.6 (2)
C61—C11—C71	120.1 (2)	C22—C12—C72	119.9 (2)
C21—C11—C71	119.9 (2)	C62—C12—C72	120.5 (2)
O31—C21—C31	116.9 (2)	O32—C22—C32	117.3 (3)
O31—C21—C11	123.9 (2)	O32—C22—C12	123.1 (3)
C31—C21—C11	119.2 (3)	C32—C22—C12	119.5 (3)

C41—C31—C21	120.4 (3)	C42—C32—C22	120.7 (3)
C41—C31—H31	119.8	C42—C32—H32	119.7
C21—C31—H31	119.8	C22—C32—H32	119.7
C31—C41—C51	119.3 (2)	C52—C42—C32	118.6 (3)
C31—C41—H41	120.4	C52—C42—H42	120.7
C51—C41—H41	120.4	C32—C42—H42	120.7
C61—C51—F11	118.6 (2)	F12—C52—C42	118.1 (3)
C61—C51—C41	122.7 (2)	F12—C52—C62	118.9 (2)
F11—C51—C41	118.6 (2)	C42—C52—C62	123.0 (3)
C51—C61—C11	118.4 (2)	C52—C62—C12	118.6 (2)
C51—C61—H61	120.8	C52—C62—H62	120.7
C11—C61—H61	120.8	C12—C62—H62	120.7
O21—C71—O11	122.6 (2)	O22—C72—O12	122.7 (2)
O21—C71—C11	121.5 (2)	O22—C72—C12	121.8 (2)
O11—C71—C11	115.9 (2)	O12—C72—C12	115.5 (2)
C61—C11—C21—O31	179.7 (2)	C62—C12—C22—O32	179.8 (2)
C71—C11—C21—O31	−1.5 (4)	C72—C12—C22—O32	−0.2 (4)
C61—C11—C21—C31	0.2 (4)	C62—C12—C22—C32	0.5 (4)
C71—C11—C21—C31	179.1 (2)	C72—C12—C22—C32	−179.6 (3)
O31—C21—C31—C41	−179.1 (2)	O32—C22—C32—C42	−179.8 (2)
C11—C21—C31—C41	0.4 (4)	C12—C22—C32—C42	−0.4 (4)
C21—C31—C41—C51	−1.1 (4)	C22—C32—C42—C52	0.1 (4)
C31—C41—C51—C61	1.3 (4)	C32—C42—C52—F12	−179.9 (2)
C31—C41—C51—F11	−177.7 (2)	C32—C42—C52—C62	0.3 (4)
F11—C51—C61—C11	178.3 (2)	F12—C52—C62—C12	179.9 (2)
C41—C51—C61—C11	−0.7 (4)	C42—C52—C62—C12	−0.2 (4)
C21—C11—C61—C51	−0.1 (4)	C22—C12—C62—C52	−0.2 (4)
C71—C11—C61—C51	−178.9 (2)	C72—C12—C62—C52	179.9 (2)
C61—C11—C71—O21	−179.1 (3)	C22—C12—C72—O22	−4.6 (4)
C21—C11—C71—O21	2.1 (4)	C62—C12—C72—O22	175.3 (2)
C61—C11—C71—O11	0.6 (4)	C22—C12—C72—O12	175.4 (2)
C21—C11—C71—O11	−178.3 (2)	C62—C12—C72—O12	−4.7 (4)

Hydrogen-bond geometry (Å, º)

D—H···A	D—H	H···A	D···A	D—H···A
O11—H11*O*···O21[i]	0.84	1.81	2.643 (3)	176
O31—H31*O*···O21	0.84	1.90	2.620 (3)	144
O31—H31*O*···F11[ii]	0.84	2.38	3.028 (3)	134
O12—H12*O*···O22[iii]	0.84	1.83	2.659 (3)	168
O32—H32*O*···O22	0.84	1.88	2.597 (3)	143
O32—H32*O*···F12[iv]	0.84	2.64	3.287 (3)	135

Symmetry codes: (i) −*x*+1, −*y*+1, −*z*; (ii) *x*, −*y*+3/2, *z*−1/2; (iii) −*x*, −*y*, −*z*; (iv) *x*, −*y*+1/2, *z*−1/2.